land

MDPI

Article

Characteristics of Spatial Correlation Network Structure and Carbon Balance Zoning of Land Use Carbon Emission in the Tarim River Basin

Zhe Gao [1], Jianming Ye [1,2,*], Xianwei Zhu [1], Miaomiao Li [1], Haijiang Wang [1] and Mengmeng Zhu [1,*]

[1] Agricultural College, Shihezi University, Shihezi 832003, China; 20222012065@stu.shzu.edu.cn (Z.G.); 20222012064@stu.shzu.edu.cn (X.Z.); limiaomiao@stu.shzu.edu.cn (M.L.); wanghaijiang@shzu.edu.cn (H.W.)
[2] School of Architecture and Urban Planning, Tongji University, Shanghai 200092, China
* Correspondence: 2110309@tongji.edu.cn (J.Y.); yjm_agr@shzu.edu.cn (M.Z.)

Abstract: An accurate understanding of the structure of spatial correlation networks of land use carbon emissions (LUCEs) and carbon balance zoning plays a guiding role in promoting regional emission reductions and achieving high-quality coordinated development. In this study, 42 counties in the Tarim River Basin from 2002 to 2022 were chosen as samples (Corps cities were excluded due to missing statistics). The LUCE spatial correlation network characteristics and carbon balance zoning were analyzed by using the Ecological Support Coefficient (ESC), Social Network Analysis (SNA), and Spatial Clustering Data Analysis (SCDA), and a targeted optimization strategy was proposed for each zone. The results of the study indicate the following: (1) The LUCEs showed an overall upward trend, but the increase in LUCEs gradually slowed down, presenting a spatial characteristic of "high in the mid-north and low at the edges". In addition, the ESC showed an overall decreasing trend, with a spatial characteristic opposite to that of the LUCEs. (2) With an increasingly close spatial LUCE correlation network in the Tarim River Basin, the network structure presented better accessibility and stability, but the individual network characteristics differed significantly. Aksu City, Korla City, Bachu County, Shache County, Hotan City, and Kuqa City, which were at the center of the network, displayed a remarkable ability to control and master the network correlation. (3) Based on the carbon balance analysis, the counties were subdivided into six carbon balance functional zones and targeted synergistic emission reduction strategies were proposed for each zone to promote fair and efficient low-carbon transformational development among the regions.

Keywords: land use carbon emission (LUCE); spatial correlation network; carbon balance zoning; Social Networking Analysis (SNA); carbon peaking and carbon neutralization

Citation: Gao, Z.; Ye, J.; Zhu, X.; Li, M.; Wang, H.; Zhu, M. Characteristics of Spatial Correlation Network Structure and Carbon Balance Zoning of Land Use Carbon Emission in the Tarim River Basin. *Land* **2024**, *13*, 1952. https://doi.org/10.3390/land13111952

Academic Editors: Xinhai Lu and Danling Chen

Received: 29 October 2024
Revised: 17 November 2024
Accepted: 17 November 2024
Published: 19 November 2024

1. Introduction

As global warming, caused by carbon emissions, is becoming increasingly serious, maintaining the balance between natural ecosystems and socio-economic systems and bringing about socio-economic transformation to achieve low carbon goals have become major issues that need to be urgently solved by all countries [1,2]. Based on this, China has put forward the strategic goal of "carbon peaking by 2030 and carbon neutrality by 2060" [3]. Existing research results show that land use alterations contribute to approximately one-third of anthropogenic carbon emissions [4,5]. Therefore, research on land use carbon emissions (LUCEs) is crucial in promoting regional carbon emission reductions and accomplishing green development.

Scholars have conducted a large number of studies on land use carbon emissions (LUCEs), with the main focuses on spatio-temporal differentiation [6–8], influencing factors [9–11], prediction simulation [12,13], and land use optimization under the low-carbon perspective [14,15]. To estimate carbon emissions, existing studies have mainly used model estimation [16], sample plot inventory [17], and the IPCC emission factor method [18].

However, due to the problems of insufficient data and difficulties in obtaining data, it is still challenging to estimate the LUCEs in a study area on a micro scale. The use of remote sensing data, such as nighttime light remote sensing data, can make up for the lack of energy data, and it provides a good solution for carbon emission calculation at the meso/micro scale [19,20]. With the deepening of China's regional coordinated development strategy, the spatial correlations of economic development, population flow, and energy consumption, as well as the activities of production factors, geographical limitations have been broken through, presenting the characteristics of a complex network structure [21–23]. By analyzing the carbon correlation network structure at the provincial and city scales, some studies have found that the current carbon emission correlation shows the spatial differentiation characteristics of "club", "vassal economy", and "gradient fault" systems, with problems such as "carbon leakage" and "carbon emission refuges" [24,25]. How to carry out carbon balance zoning and formulate regional synergistic emission reduction action programs has increasingly become a research hotspot [26–28].

The Tarim River Basin is one of the driest and most ecologically fragile regions in China and even in Eurasia [29,30]. With rapid economic development, the ever-increasing area of artificial oases, irrational land allocation, and aggravated soil desertification have led to an increasing amount of non-essential carbon emissions, as well as an increasingly prominent contradiction between social development and regional ecology [31–33]. There are significant regional differences in economic development, energy endowment, and ecological pressure within the Tarim River Basin [34,35]. As inter-regional exchanges and cooperation increase, spatial correlation formed has a crucial impact on the flow of carbon emission factors.

Based on the abovementioned research findings, we proposed two key research objectives for this study. First, on the basis of LUCE measurement, the role characteristics of each research unit in the LUCE spatial correlation network were identified using Social Network Analysis (SNA). Second, this study utilized LUCE spatial agglomeration, the Ecological Support Coefficient (ESC), and spatial correlation network structure to delineate carbon balance zoning. This analysis emphasized the internal spatial correlation within LUCE balance zoning and enhanced the scientific and empirical basis for zoning planning.

2. Materials and Methods

2.1. Study Area

The Tarim River Basin (73°10′–94°05′ E, 34°55′–43°08′ N) is located in the southern region of Xinjiang Uygur Autonomous Region [36]. The landscape pattern of the basin consists of mountains, glaciers, valley steppes, and oases, with deserts dominating the landscape [37,38]. Because of the extremely fragile ecological environment and the favorable geographic location in the core area of the Silk Road, the economic development status and ecological environment maintenance of the basin occupy an important position in Xinjiang [39]. The Corps cities were not included in the study area due to missing statistics. The study area is shown in Figure 1.

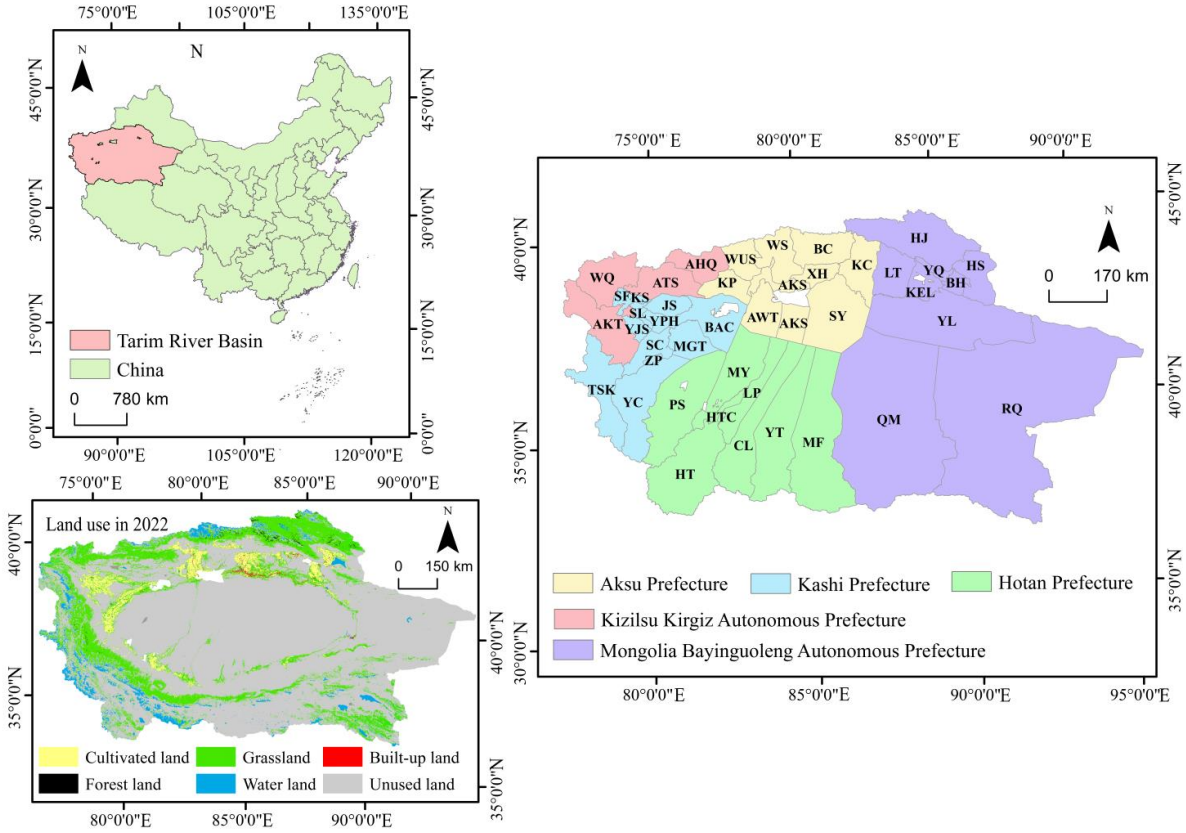

Figure 1. Overview of the study area. Note: AHQ, AKS, AKT, ATS, AWT, BC, BAC, BH, CL, JS, HJ, HS, HTC, HT, KS, KP, KC, KEL, LT, LP, MGT, MF, MY, PS, QM, RQ, SY, SC, SF, SL, TSK, YL, WS, WQ, WUS, XH, YQ, YC, YJS, YT, YPH, and ZP represent Aheqi, Aksu, Aketao, Atushi, Awati, Bachu, Baicheng, Bohu, Cele, Jiashi, Hejing, Heshuo, Hotan City, Hotan, Kashi, Keping, Kuche, Korla, Luntai, Luopu, Maigaiti, Minfeng, Moyu, Pishan, Qiemo, Ruoqiang, Shaya, Shache, Shufu, Shule, Taxkorgan Tajik Autonomous County, Yuli, Wensu, Wuqia, Wushi, Xinhe, Yanqi Hui Autonomous County, Yecheng, Yingjisha, Yutian, Yuepuhu, and Zepu, respectively. The map was constructed based on a standard map produced by China's Ministry of Natural Resources (MNR) using the standard map service website (review map number GS(2022)4314), with no modifications to the base map.

2.2. Data Sources

Four main types of data were used in this study: namely, land use data, energy carbon emission data, nighttime lighting data and social statistics data (Table 1).

Table 1. Data sources and descriptions.

Data Name	Data Sources	Data Declaration
Land use data	"30 m annual land cover and its dynamics in China from 1990 to 2022" http://www.ncdc.ac.cn/portal/metadata/9de270f3-b5ad-4e19-afc0-2531f3977f2f (accessed on 4 September 2023)	The resolution is 30 m × 30 m, and the land use is categorized into six types: cultivated land, forest land, grassland, water land, built-up land, and unused land through the reclassification function of GIS.
Energy carbon emissions data	"County-level CO_2 emissions and sequestration in China during 1997–2017" https://doi.org/10.6084/m9.figshare.13090370 (accessed on 25 September 2023)	The carbon emission results from this dataset have a good fit of 0.998 with the results obtained from energy accounting.
Nighttime lighting data	"Developing improved time-series DMSP-OLS-like data (1992–2022) in China by integrating DMSP-OLS and SNPP-VIIRS" https://ieeexplore.ieee.org/document/9652530 (accessed on 28 September 2023)	The resolution is 1 km × 1 km. The biggest advantage of this dataset is that it realizes the calibration, synthesis and improvement of the long time series of nighttime light data in China.
Social statistics data	https://data.cnki.net (accessed on 10 July 2023)	Missing data were filled in by multiple interpolation method.

2.3. Research Methods

First, this study analyzed LUCEs and the ESC in the Tarim River Basin using land use data and other related data. Then, with the help of SNA, we explored the characteristics of the LUCE spatial network structure from both the individual and overall network perspectives. In addition, by combining the ESC, spatial agglomeration, and spatial network structure, the carbon balance partition was established and differentiated emission reduction strategies were proposed. A detailed analysis workflow is shown in Figure 2.

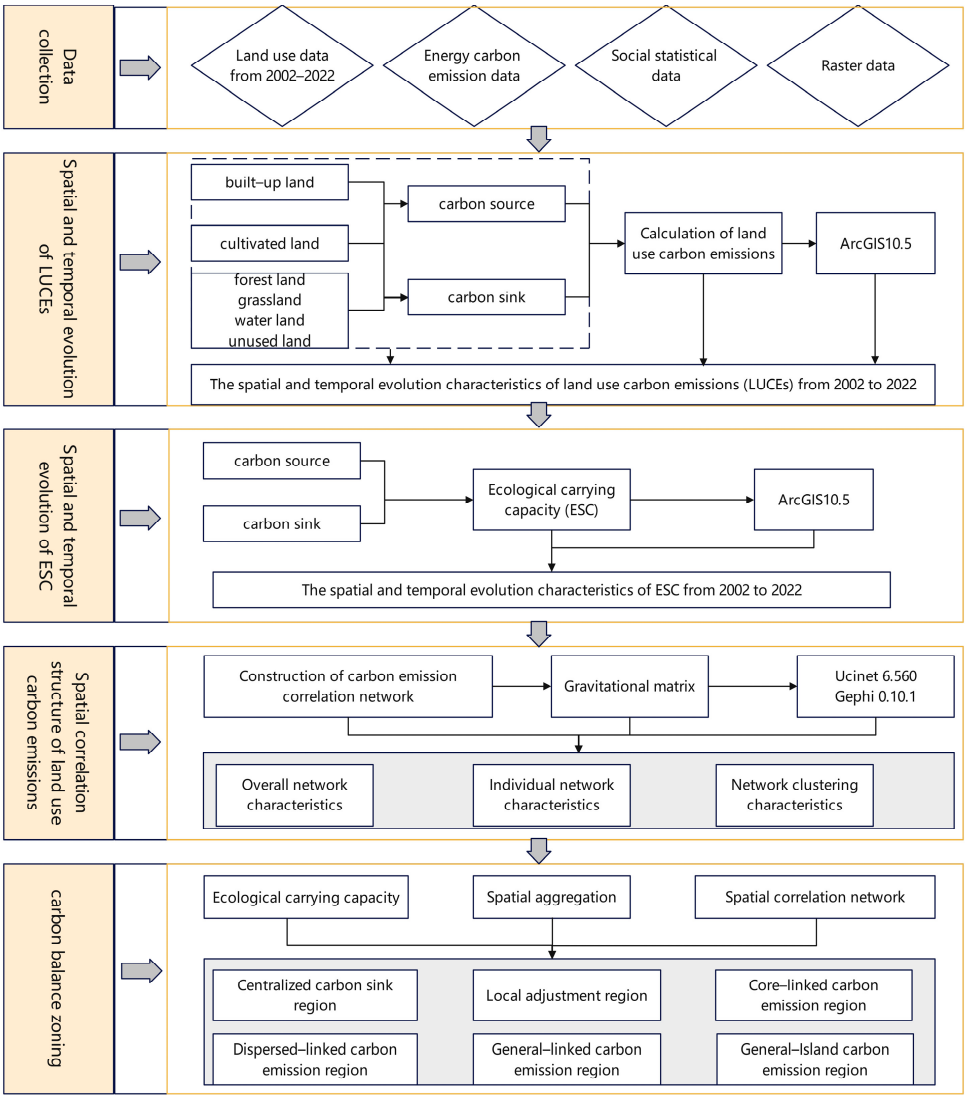

Figure 2. Flow chart of study.

2.3.1. LUCE Measurement Methodologies

LUCEs are equal to the sum of carbon emissions/absorptions of each land use type [40]. Among the land use types, built-up land belongs to carbon sources; forest land, grassland, water land, and unused land belong to carbon sinks; and cultivated land has both carbon source and carbon sink attributes, as shown in Equation (1).

$$C = E_c + E_a + E_x \quad (1)$$

where C is the LUCE amount; E_c is carbon emissions from built-up land; E_a is carbon emissions from cultivated land; and E_x is carbon absorption from cropland, woodland, grassland, watersheds, and unused land.

(1) Built-up land carbon emissions

Built-up land carbon emission values, as anthropogenic carbon emissions generated during land use activities, can be indirectly obtained from the energy carbon emissions generated by built-up land as it hosts human production activities [41]. However, the county energy carbon emission dataset [42] has a certain lag. Considering the correlation between carbon emissions and nighttime lighting data, we fitted the nighttime lighting data of each county to the data on carbon emissions from energy consumption in the corresponding year, and the equation with the highest goodness-of-fit (Table 2) was selected to estimate the energy carbon emission of each county in 2018, 2019, 2020, 2021, and 2022.

Table 2. Fitting results of energy carbon emissions by counties in the Tarim River Basin.

County	Fitted Model	R^2	County	Fitted Model	R^2
Korla	$=19.039x^{1.286}$	0.825	Bachu	$=143.195x^{1.001}$	0.854
Luntai	$=127.613x + 6.879$	0.861	Taxkorgan	$=46.372x + 0.008$	0.925
Yuli	$=e^{1.296-(0.002/x)}$	0.879	Hotan City	$=-0.100 + 1.050x - 0.104x^2$	0.920
Ruoqiang	$=3.448 + 0.336\ln x$	0.877	Hotan	$=e^{0.504-0.001/x}$	0.980
Qiemo	$=8.926 - 0.007/x$	0.843	Moyu	$=4.423 + 0.581lnx$	0.846
Yanqi	$=8.084x + 1.096$	0.902	Pishan	$=35.782x^{0.685}$	0.949
Heshuo	$=0.0179x^{0.591}$	0.924	Luopu	$=4.111 + 0.549lnx$	0.936
Bohu	$=7.000x^{0.630}$	0.922	Cele	$=86.731x^{0.883}$	0.888
Aksu	$=-0.460 + 50.760x - 63.039x^2$	0.801	Kuche	$=3.036 - 70.283x + 507.838x^2 - 849.570x^3$	Kuche
Yutian	$=72.787x^{0.918}$	0.966	Minfeng	$=273.203x + 0.080$	0.865
Wensu	$=4.136x^{0.242}$	0.909	Wushi	$=7.983x^{0.652}$	0.913
Shaya	$=14.861 + 3.246lnx$	0.834	Awati	$=97.841x^{1.037}$	0.833
Xinhe	$=4.418 + 0.746lnx$	0.976	Keping	$=71.186x + 0.009$	0.963
Baicheng	$=76.492x^{1.196}$	0.911	Atushi	$=24.621x^{0.831}$	0.931
Maigaiti	$=0.120 + 103.522x - 681.512x^2$	0.859	Aketao	$=e^{-0.518-0.001/x}$	0.963
Yingjisha	$=-0.124 + 42.738x - 590.340x^2 + 2502.028x^3$	0.921	Aheqi	$=0.011 + 78.413x - 6402.445x^2 + 178{,}804.289x^3$	0.963
Jiashi	$=18.517x^{0.813}$	0.872	Wuqia	$=e^{0.441-0.003/x}$	0.928
Yupuhu	$=0.055 + 21.913x - 47.306x^2$	0.959	Kashi	$=2.391x - 6.636$	0.858
Zepu	$=-0.780 + 9.884x - 5.696x^2$	0.978	Shufu	$=7.794x^{0.648}$	0.906
Shache	$=-0.068 + 72.571x - 330.731x^2$	0.939	Shule	$=-0.0385 + 8.160x + 0.350x^2$	0.989
Yecheng	$=e^{2.170-0.011/x}$	0.946	Heshuo	$=22.876x^{0.602}$	0.883

(2) Cultivated land carbon emission

Cultivated land carbon emission mainly comes from agricultural production activities, such as the application of fertilizers and pesticides, agricultural plastic film, agricultural machinery, tillage, and irrigation, as well as from CH_4 produced during crop cultivation [43]. The equation for calculating cultivated land carbon emission is as follows:

$$E_a = \sum_{i}^{n} S_i \times \beta_i + \sum_{j}^{m} A_j \times \gamma_j \quad (2)$$

where E_a is the cultivated land carbon emission; S_i is the amount of resources used in an area for each type of agricultural activity; β_i is the carbon emission coefficient of each type of cultivated land utilization activity; A_j is the planting area of each crop; and γ_j is the carbon emission coefficient of each crop type in the whole growth process. Combining the research findings of previous scholars and the actual utilization of arable land in the Tarim River Basin [44–48], carbon emission sources in the process of arable land utilization were classified into five categories: chemical fertilizer, pesticide, agricultural plastic film, organic carbon loss from tilling, and electric energy consumption from agricultural irrigation. The crops with the largest planting area in Xinjiang, namely, cotton, wheat, maize, soybeans, vegetables, and rice, were used for the measurement of carbon emission. According to previous studies, the relevant carbon emission coefficients are shown in Table 3.

Table 3. Carbon emission coefficient of cultivated land.

Carbon Emission Source	Carbon Emission Factor	Carbon Emission Coefficient
Agricultural land use	Tillage	312.6 kg(C)/hm^2
	Irrigation	266.48 kg(C)/hm^2
	Fertilizers	0.8956 kg(C)/kg
	Pesticides	4.9341 kg(C)/kg
	Agricultural plastic film	5.18 kg(C)/kg
	Agricultural machinery	0.1802 kg(C)/kw
Crops planting	Cotton	1493.16 kg(C)/hm^2
	Wheat	142.22 kg(C)/hm^2
	Maize	205.78 kg(C)/hm^2
	Soybean	186.10 kg(C)/hm^2
	Vegetable	401.80 kg(C)/hm^2
	Rice	717.46 kg(C)/hm^2

(3) Carbon absorption of cultivated land, forest land, grassland, water land, and unused land

In this study, carbon absorption of cultivated land, forest land, grassland, water land, and unused land was estimated using the carbon emission factor method [49]. The formula is as follows:

$$E_x = \sum_{m=1}^{n} (S_m \times i_m) \quad (3)$$

where n is the land use type; S_m is the area of every land use type; and i_m is the carbon emission coefficient of each land use type. Combining the findings from previous studies and the natural geography of the Tarim River Basin [50–52], the carbon absorption coefficients (kg©/(m^2·a)) of cultivated land, forest land, grassland, water land, and unused land in this study were taken to be −0.0007, −0.0635, −0.0390, −0.0248, and −0.0005, respectively.

2.3.2. Spatial Correlation Network Analysis of LUCE

(1) Spatial correlation network construction of LUCE

The gravitational model is derived from the law of gravity in physics and has been widely used in the field of spatial interactions, including to explore LUCE correlations in watersheds [53,54]. To better reflect the degree of LUCE correlation among the counties in the basin, we introduced carbon emissions, gross domestic product (GDP), and the parameter k into the model with the following equation [55]:

$$y_{ij} = k_{ij} \times \frac{\sqrt[3]{P_i C_i G_i}\sqrt[3]{P_j C_j G_j}}{\left(\frac{D_{ij}}{e_i - e_j}\right)^2}, \; k_{ij} = \frac{C_i}{C_i + C_j} \quad (4)$$

where y_{ij} and D_{ij} are the gravitational force and spatial distance between county i and county j, respectively; P, C, G, and e denote a county's year-end population, carbon emissions, gross domestic product, and per capita income level, respectively; and k_{ij} denotes the gravity coefficient of carbon emissions from county i to county j. To avoid weak spatial linkage affecting the results, based on previous related studies, we took the row mean value of the matrix as a threshold and assigned 1 to a gravitational value greater than the mean value, whereas a lower-than-mean value was assigned 0; this allowed us to construct a bivariate matrix characterizing the correlation relationship of LUCEs among the counties.

(2) Structure characteristics of the LUCE spatial correlation network

Social Network Analysis (SNA) quantitatively analyzes the association paths between nodes in the form of a network and identifies the role of each node [56]. Therefore, we used SNA to analyze the overall, individual, and cluster structure characteristics of the LUCE spatial correlation network. The network density, network connection degree, and

network hierarchy degree can well portray the overall characteristics; the degree, closeness, and betweenness centrality can well portray the individual characteristics; and the block model can be used to analyze the spatial clustering characteristics. According to the evaluation methods used by other scholars [57,58], we categorized the spatial network structure into four types: (1) bidirectional overflow blocks, where there are overflow relationships to other blocks as well as overflow to the intra-block, but overflow received from other blocks occurs less often; (2) net spillover blocks, where block members present fewer receiving relationships from other blocks than those overflowing to other blocks; (3) primary beneficiary blocks, where there is a much larger number of receiving relationships than overflow relationships, as well as overflow relationships between members within the block; and (4) agent blocks, where there is a much larger number of receiving and overflowing relationships, with blocks' members playing the role of bridges in the network.

2.3.3. Exploratory Spatial Data Analysis

Exploratory spatial data analysis identifies agglomeration effects by exploring and outlining the spatial distribution of elements or phenomena, which mainly includes global spatial autocorrelation and local spatial autocorrelation [59]. The formula for calculating global spatial autocorrelation is as follows:

$$I = \frac{m\sum_{i=1}^{m}\sum_{j=1}^{m} W_{ij}\left(C_i - \overline{C}\right)\left(C_j - \overline{C}\right)}{\sum_{i=1}^{m}\sum_{j=1}^{m} W_{ij}\left(C_i - \overline{C}\right)^2} \quad (5)$$

where I is the Moran index; m is the number of counties; C_i and C_j are the LUCEs of county i and county j, respectively; and W_{ij} is the spatial weighting matrix.

Local spatial autocorrelation is usually used to analyze the local spatial clustering or divergence characteristics of a research unit, which is calculated using the following formula:

$$I_i = \frac{m\left(C_i - \overline{C}\right)\sum_{i=1}^{m} W_{ij}\left(C_j - \overline{C}\right)}{\sum_{i=1}^{m}\left(C_j - \overline{C}\right)} \quad (6)$$

where I_i is the Anselin local Moran's I index. If I_i is greater than 0, it means that the carbon emissions of a county and its neighboring county are similar, so the spatial agglomerations can be classified into high–high (HH) and low–low (LL) clusters; if I_i is less than 0, it means that the carbon emissions of the county and its neighboring county are significantly different, so the spatial agglomerations can be classified into high–low (HL) and low–high (LH) clusters.

2.3.4. Ecological Support Coefficient (ESC)

ESC reflects the magnitude of the carbon sink capacity in the study area [60]. The formula is as follows:

$$ESC = \frac{C_{ni}/C_n}{C_{ri}/C_r} \quad (7)$$

where ESC is the Ecological Support Coefficient of LUCEs in the study area; C_{ni} and C_{ri} are the carbon sink and carbon source of county i, respectively; and C_n and C_r are the carbon sink and carbon source of the Tarim River Basin, respectively. If ESC is greater than 1, it indicates that the carbon sink capacity of the study area is strong; if ESC is less than 1, it indicates that the carbon sink capacity of the area is weak.

3. Results

3.1. Spatio-Temporal Evolution Characteristics of LUCEs in the Tarim River Basin

As illustrated in Figure 3, the LUCE in the Tarim River Basin increased significantly, with an increase from 1152.38 $\times$ 10^4 t in 2002 to 17,212.49 $\times$ 10^4 t in 2022. The average annual growth rate of LUCE decreased significantly, with a decrease from 34.53% in 2002 to 11.34% in 2022; the carbon emission intensity increased from 2.81 t/million CNY in

2002 to 3.64 t/million CNY in 2022. In terms of carbon source, built-up land played the most important role, accounting for more than 93% of carbon emissions, with a growth of 15,825.74 × 10^4 t during 2002–2022; carbon emissions from cultivated land were another source, rising from 135.91 × 10^4 t in 2000 to 203.39 × 10^4 t in 2022. In terms of carbon absorption, grassland made the highest contribution, accounting for more than 83% of carbon absorption; therefore, grassland was the most important carbon sink, followed by unused land, while forest land and water contributed weakly to carbon absorption. Overall, the absorption of the carbon sink was significantly lower than the emission from carbon sources. Therefore, the LUCEs in the Tarim River Basin are expected to continue to rise in the coming period, and it is difficult to offset the rise in carbon emission from built-up land through the absorption of carbon sink land only.

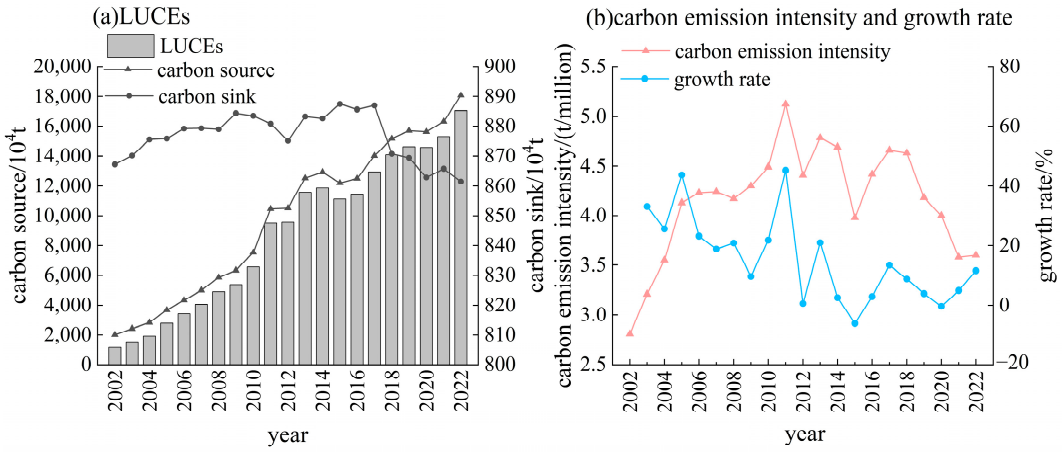

Figure 3. Changes in land use carbon emissions (LUCEs) in the Tarim River Basin.

In terms of spatial distribution (Figure 4), the LUCE was higher in Kuqa City, Korla City, Luntai County, Shaya County, and Aksu City. The dual drive of urbanization and industrialization had resulted in rapidly expanding construction land and dense population in these counties, which are located in the hinterland of Xinjiang. This led to their LUCE growth. The LUCEs were smaller in Ahechi, Aktau, and Tashkurgan Tajik Autonomous County because of the relatively slow economic development of these counties, resulting in less energy consumption.

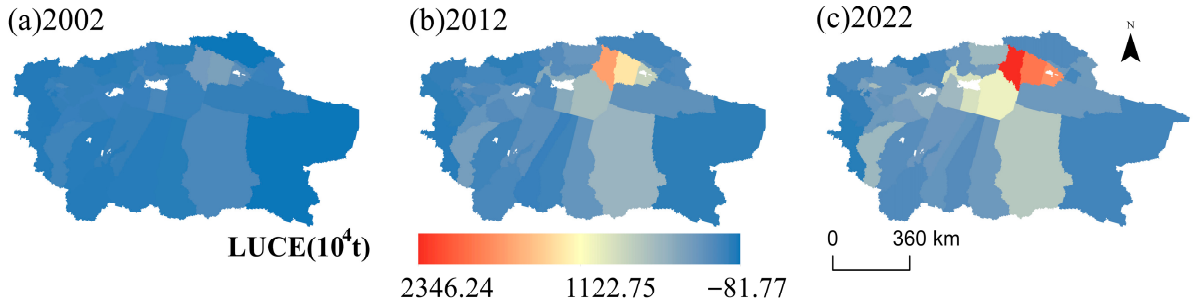

Figure 4. Spatial distribution of LUCE in the Tarim River Basin.

3.2. Spatio-Temporal Distribution Characteristics of ESC

With the decline in overall ESC in the study area, the spatial difference in ESC was evident, characterized by being "low in the middle and high at the edge" (Figure 5). In 2002, the areas with high values of ESC were distributed in the western regions such as Tashkurgan Tajik Autonomous County and Wuqia County, as well as Ruoqiang County in the east. These counties, with their major industries based on agriculture, had a strong carbon sink capacity due to their underdeveloped economies, large areas of carbon sink land, and rich ecological resources. In 2012, the ESC decreased significantly, indicating that

the rapid economic development and urbanization process aggravated ecological pressure. In 2022, the decreasing trend of ESC slowed down. Compared with 2002, there were fewer regions with ESC < 1.00 and ESC > 20.00. Ecological environmental protection was emphasized in the context of Beautiful China construction, thus contributing to this result.

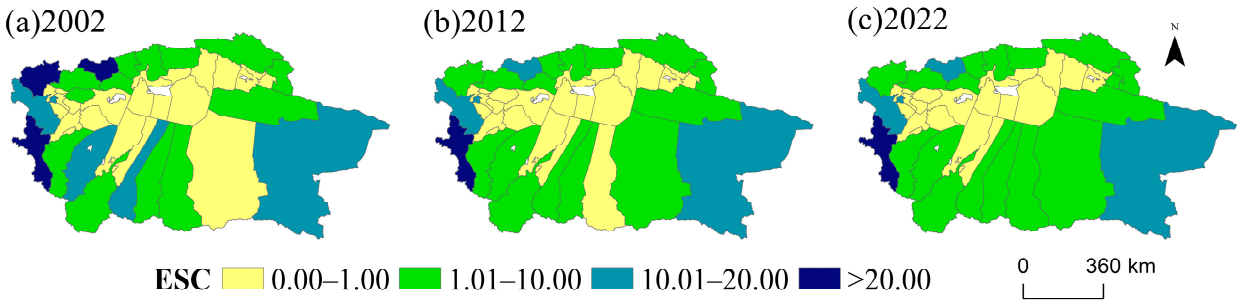

Figure 5. Spatio-temporal evolution of the Ecological Support Coefficient (ESC) in the Tarim River Basin.

3.3. Structure of the LUCE Spatial Correlation Network in the Counties of Tarim River Basin

3.3.1. Overall Characterization of the LUCE Spatial Correlation Network

According to Equation (4), we constructed a graph of the LUCE correlation intensity in the Tarim River Basin in 2002, 2012, and 2022 (Figure 6). Overall, the network correlation and network stability of LUCE increased in the basin, and the overall network structure was characterized by a "core-edge" structure. From the perspective of spatial distribution, the spatial correlation of the north-central region was strong. Because of the developed economy and convenient transportation, the node counties represented by Aksu, Hotan, Kashgar, Korla, Bachu, Bohu, and Aheqi counties played a "dominant" role in the network and had a significant relationship with other counties. From the perspective of network density changes, the densities in 2002, 2012, and 2022 were 0.1678, 0.3264, and 0.3310, respectively, indicating a strengthening of LUCE interaction links between counties; the slowing down of the network density growth rate in the later period might be due to the faster development of transportation facilities and information networks, and the more frequent exchanges of LUCE-related elements from 2012 to 2022. However, the increase in element exchange also brought about an increase in the gravitational mean value between nodes, which made the determination of the spatial correlation relationship between network nodes more difficult. In addition, the network correlation of the basin was overall 1, reflecting a closely connected and robust spatial correlation network of LUCEs. The network hierarchy degree decreased from 0.51 in 2002 to 0.39 in 2019, suggesting that the spatial correlation network was less dependent on a single node or a few nodes.

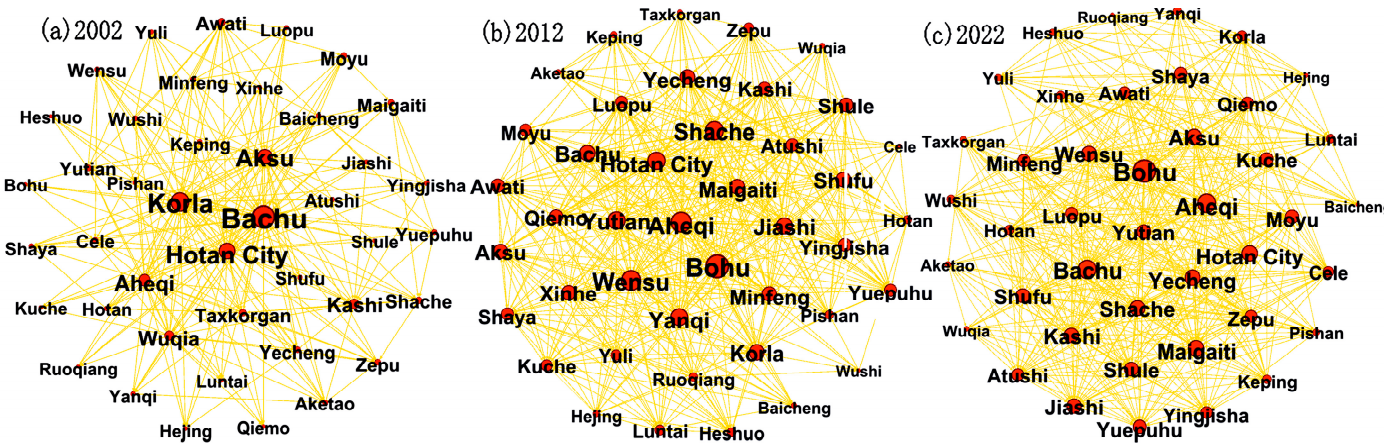

Figure 6. Evolution of the spatial correlation network structure of LUCE in the Tarim River Basin.

3.3.2. Individual Characterization of Spatial Correlation Network

Using UCINET6.560, we determined the degree, closeness, and betweenness centrality of the LUCE correlation network (Figure 7). In terms of degree centrality and closeness centrality, counties at the relative center of the correlation network performed better, such as Aksu City, Bachu County, Kuqa City, Korla City, Kashgar City, Gashi County, and Hotan City, and they were able to quickly form connection with other regions. In addition, their higher in-degree centrality indicated that these counties received more carbon overflow from other counties. Among them, the in-degree centralities of Aksu City and Korla City were significantly higher than those of other counties, which fully demonstrated their central role in the correlation network. In terms of out-degree centrality, counties such as Bachu County, Aheqi County, Hotan City, Bohu County, Minfeng County, Yutian County, and Qiemo County had long been in the top ten, indicating that they generated a high amount of carbon emission overflow. On the one hand, regions with better economic development, such as Bachu County and Hotan City, could attain carbon transfer through the path of industrial transfer and economic cooperation, in addition to absorbing advantageous factors internally. On the other hand, under the siphoning effect of developed counties, the overflow of human resources, backward infrastructure development, and further geographic–economic distance growth in the edge counties, such as Aheqi, Bohu, Minfeng, Yutian, and Qimo counties, hindered the inflow of capital, talent, technology, and other factors, and it was difficult for these counties to quickly establish carbon connection with other regions.

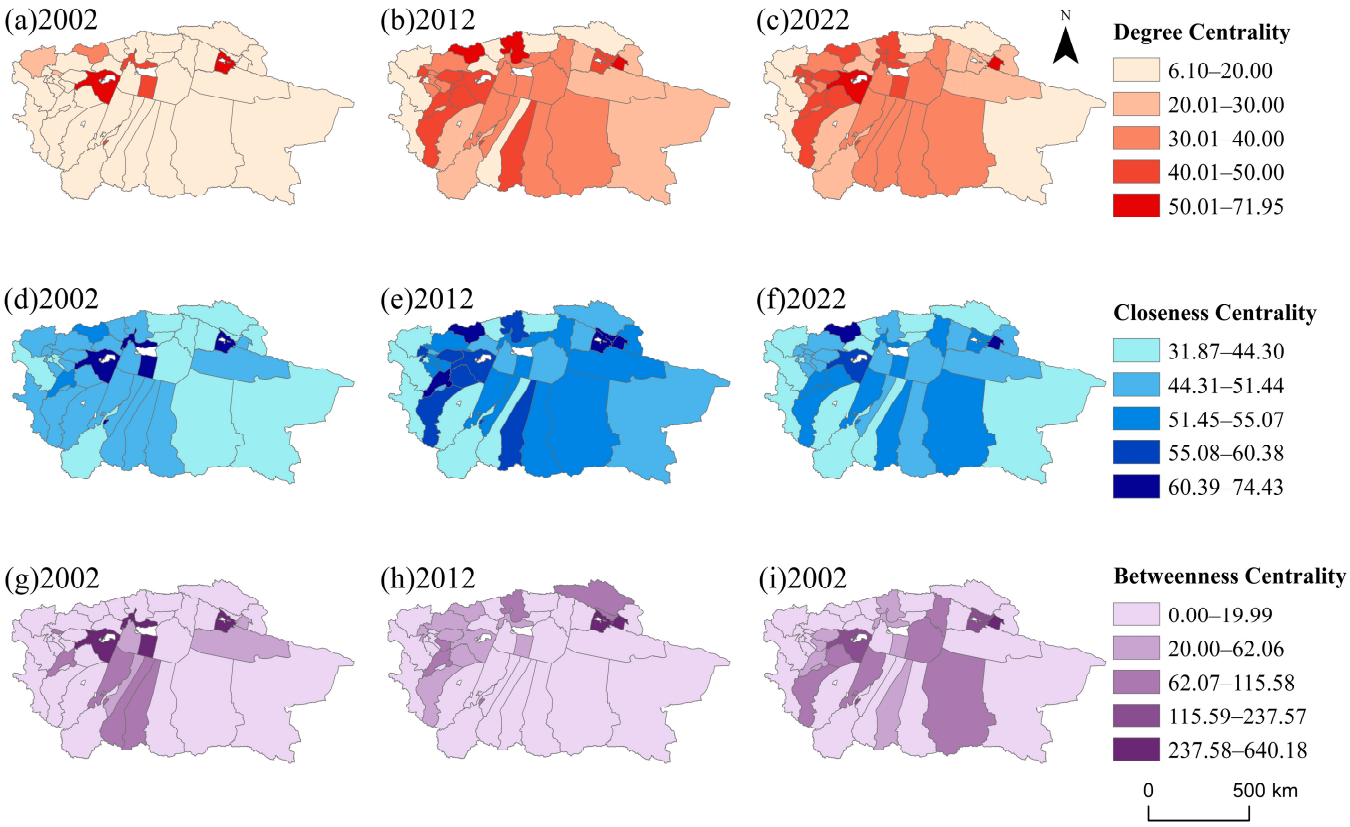

Figure 7. Individual characteristics of the LUCE spatial correlation network in the Tarim River Basin.

In terms of betweenness centrality, the regions in the top ten were increasingly concentrated in counties with a better economic base, with Aksu City, Korla City, Bachu County, Shache County, Hotan City, and Kuqa City being consistently located in the paths with more nodes. These counties had a high degree of factor marketization, more active trading of carbon emission rights and land indexes, and more smooth and convenient factor flows,

which were more likely to affect the LUCE of neighboring regions through the overflow of low-carbon technologies and green production lifestyles.

3.3.3. Clustering Characteristics of the Spatial Correlation Network

As can be seen from Table 4, the spatial overflow effect of LUCE was mainly dominated by inter-regional overflow, indicating that the spatial correlation between blocks was greater than the spatial correlation within blocks. In terms of spatial distribution, the panels comprising the southern and western regions were the main exporters of elements in most years, while the panels comprising the northern districts and counties were the main receivers of elements in most years. The reason was that the division of blocks within the network was affected by many factors, such as geographic location and the influence of economic development, which affected the flow of various types of factors. The region consisting of Korla City, Aksu City, and Kashi City had a developed economy and convenient transportation, which made it easy to absorb all kinds of factors, thus becoming the main receiver of these factors.

Table 4. Spatial correlation of LUCEs across different geographic blocks.

Year	Block	Counties	Accepted Relationships		Overflow Relationships		Expected Internal Relationships (%)	Actual Internal Relationships (%)
			In	Out	In	Out		
2002	Net overflow	AHQ, WQ, HTC, BAC, TSK	11	22	11	120	9.76	8.40
	Bidirectional overflow	MY, SC, SF, SL, AWT, MGT, WS, YJS, ATS, LP, JS, MF, YPH	15	47	15	57	29.27	20.83
	Primary beneficiary	AKS, XH, LT, KC, HS, BH, QM, YQ, SY, BC, KEL, YL, RQ, HJ	27	105	27	8	31.71	77.14
	Agent	AKT, CL, WUS, HT, KP, YC, PS, YT, KS, ZP	4	59	4	48	21.95	7.69
2012	Net overflow	AHQ, MF, BH, QM, RQ, KP, CL, WUS, HJ, YT	36	8	36	180	21.95	16.67
	Bidirectional overflow	WS, LT, BC, AKS, XH, SY, KC, HS, AWT, YL, YQ	74	92	74	61	24.39	54.81
	Net overflow	YC, AKT, TSK, HTC, PS, HT, WQ, BAC	16	54	16	92	17.07	14.81
	Agent	MGT, KEL, LP, JS, SF, MY, KS, ATS, SC, YJS, SL, YPH, ZP	11	200	11	95	29.27	10.38
2022	Net overflow	AHQ, MF, BH, QM, RQ, HJ, BC, YT	25	7	25	160	17.07	13.51
	Primary beneficiary	KEL, LT, SY, AKS, XH, YQ, KC, HS, YL	48	104	48	17	19.51	73.85
	Agent	HTC, AKT, HT, CL, TSK, WUS, PS, WS, YC, WQ, KP	22	46	22	166	24.39	11.70
	Bidirectional overflow	MGT, AWT, JS, LP, MY, SF, ATS, KS, BAC, SC, YJS, SL, YPH, ZP	113	207	113	21	31.71	84.33

In terms of temporal evolution, in 2002, the total number of plate relationships was 290, with the north-central counties along the mainstem of the Tarim River being the main beneficiary blocks and the edge counties being the main blocks of factor overflow. The reason for the numerical growth might be that the counties disseminated their capital, technology, and experience to neighboring counties, with advancement in their own development, thus influencing the land use patterns and energy consumption of their neighbors. In 2022, the total number of plate relationships grew to 572, reflecting a further increase in the attractiveness of the core cities, with the accumulation and siphoning effects becoming more pronounced.

3.4. Spatial Optimization of Carbon Balance Zoning in the Tarim River Basin

First, we determined the carbon balance large region. Based on the calculation of ESC, the Tarim River Basin was divided into two types of areas: overall carbon sink regions and overall carbon emission regions. Then, by superimposing the empirical results of the spatial autocorrelation and spatial correlation network, we divided the carbon balance large region into six types of carbon balance functional zones (Figure 8): centralized carbon sink region, local adjustment region, core–linked carbon emission region, dispersed–linked

carbon emission region, general–linked carbon emission region, and general–island carbon emission region. The basis for the carbon balance zoning is shown in Table 5.

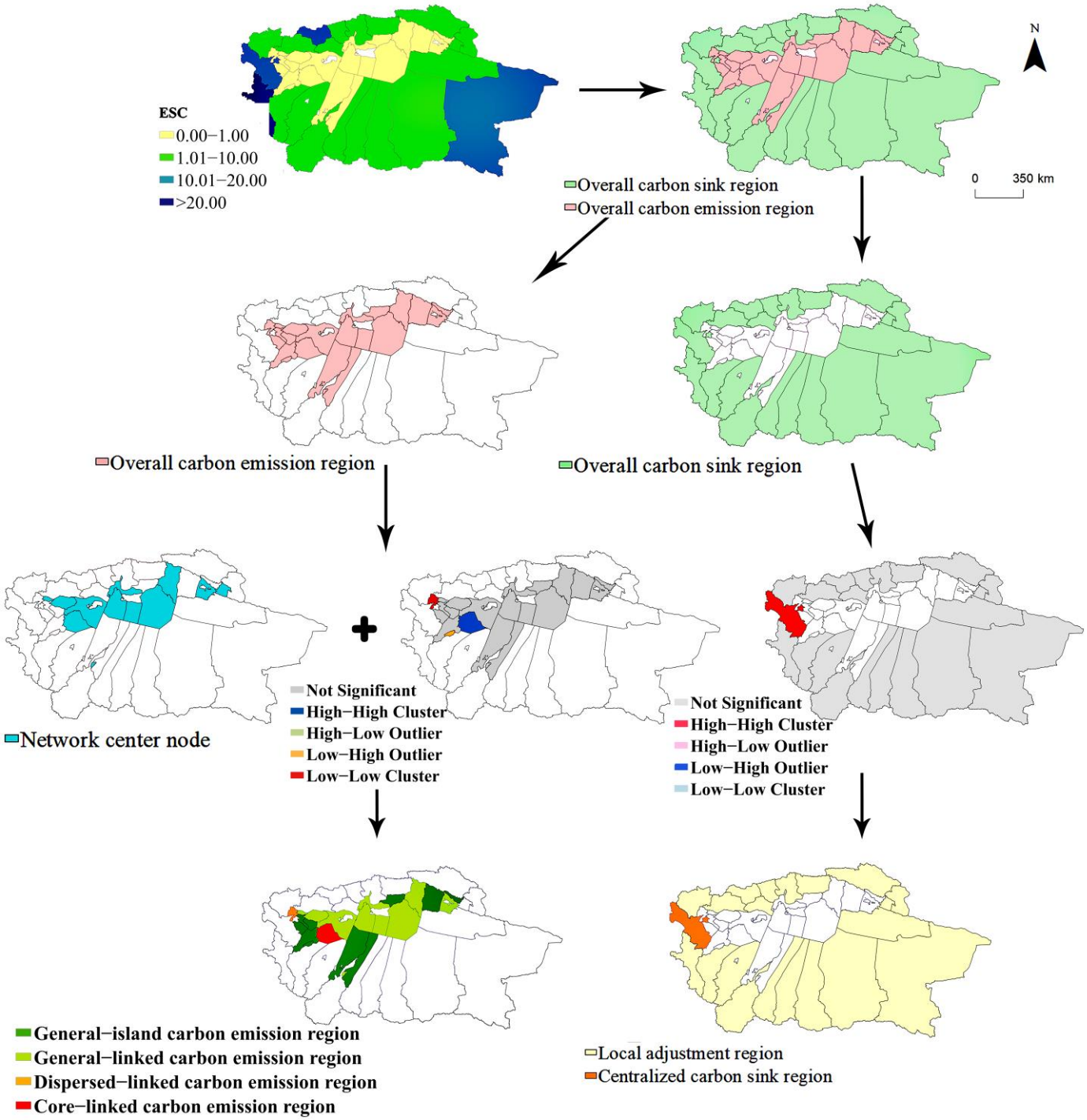

Figure 8. Carbon balance zoning in the Tarim River Basin.

Table 5. Basis of carbon balance zoning.

Carbon Balanced Large Region	Carbon Balance Functional Region	Criteria for Regionalization	County
Overall global carbon sink region	Centralized carbon sink region	ESC > 1, and belonging to the carbon sink H-H clustering area	Aketao County
	Local adjustment region	ESC > 1, and belonging to areas outside the H-H clustering of carbon sinks	Aheqi County, Atushi City, Baicheng County, Bohu County, Cele County, Hejing County, Heshuo County, Hotan County, Koping County, Minfeng County, Pishan County, Qiemo County, Ruoqiang County, Tashkurgan Tajik Autonomous County, Yuli County, Wensu County, Wuqia County, Wushi County, Yecheng County, Yutian County
Overall carbon emission region	Core–linked carbon emission region	ESC < 1, Both belonging to the carbon emission H-H clusters and to the network center nodes	Maigaiti County
	Core–island carbon emission region	ESC < 1, Belonging to carbon emission H-H clusters, but not to the network core nodes	This type of area does not exist in the study area.
	Dispersed–linked carbon emission region	ESC < 1, Both belonging to the carbon emission L-L clusters and to the network center nodes	Shufu County
	Dispersed–island carbon emission region	ESC < 1, Belonging to carbon emission L-L clusters, but not to the network core nodes	This type of area does not exist in the study area.
	General–linked carbon emission region	ESC < 1, Not belonging to the carbon emissions H-H or L-L clusters, but belonging to the network core nodes	Aksu City, Awati County, Bachu County, Jiashi County, Hotan City, Kashi City, Kuche City, Korla City, Shaya County
	General–island carbon emission region	ESC < 1, Not belonging to the carbon emissions HH or LL clusters, nor to the network core nodes	Luntai County, Lopu County, Moyu County, Shache County, Shule County, Xinhe County, Yanqi Hui Autonomous County, Yingjisha County, Yupu Lake County, Zephyr County

The characteristics of each region were as follows: (1) The area of the centralized carbon sink region accounted for 2.35% of the whole region. This region had a large amount of carbon sink land, a more prominent carbon sink function than carbon source function, and a higher ESC, and, thus, it undertook important ecological functions. In the LUCE spatial correlation network, Aketao County showed absorption of carbon emissions from other counties, which was conducive to alleviating the carbon pressure in the basin. (2) The area of the local adjustment region accounted for 78.05% of the whole region. Its regional carbon sink function was relatively strong, but the absolute amount of carbon sink was relatively limited. This region had a low degree of development of secondary and tertiary industries, cruder methods of energy utilization, and a slower pace of economic development, and it mainly contained counties with a focus on agricultural production, such as Aheqi, Hotan, Minfeng, and Ruoqiang counties. However, these counties were located around the economic growth poles of Aksu City, Korla City, and Kashi City, and showed spillover effects in the LUCE spatial correlation network, thus acting as linkages. (3) The core-linked carbon emission region had a relatively small area, accounting for 1.06% of the whole region. Maigaiti County, located in the transportation hub of the Tarim River Basin, undertook the transfer of elements between Kashi City and Aksu City. Therefore, it had a strong carbon emission function, showed significant spatial agglomeration and correlation, and belonged to the region with the most intensive and active carbon emission activities. (4) The area of the dispersed–linked carbon emission region accounted for 0.26% of the whole region. With a large area of forest land and grassland and weak intensity of human production activities, Shushi County had low overall carbon emissions. Located around Kashi City, Shufu County undertook the transfer of carbon emission factor resources between the Kizilsu Kyrgyz Autonomous Prefecture and Kashi Region, so it acted as a network hub in the correlation network. (5) The area of the general-linked carbon emission region accounted for 13.72% of the whole region. With developed heavy industries, this region had much higher carbon emissions than carbon absorption, a low ESC, and a closer correlation of carbon emission activities with other counties. In the carbon emission

network, Aksu City and Korla City attracted the inflow of labor, information technology, capital, and other factors from other regions due to their good economic fundamentals, becoming the dominant beneficiaries in the network. (6) The area of the general–island carbon emission region accounted for 4.55% of the whole region. This region had neither a clustering effect on carbon emission activities nor a core area integrated into the carbon emission network. Therefore, it was difficult for this region to perceive changes in the carbon emission behavior of other counties, and its ability to reduce carbon emissions on its own was weak.

4. Discussion

4.1. Spatial and Temporal Evolution of LUCE Spatial Correlation Network

In this study, we found that the LUCEs in the Tarim River Basin showed a general trend of "high in the north-central part and low at the edge", which was consistent with the results of Zhang et al. [51]. North-central counties had more energy resources, more developed economies, and denser populations, which led to an increase in carbon emissions, with the LUCEs exceeding 18 million tons in 2022 in Aksu City and Korla City. From 2002 to 2012, the growth rate of LUCEs in each county was relatively fast. In the context of the Western Development Policy, a large number of industries and capitals converged. This promoted economic development and increased human activities (e.g., industrial production, energy consumption, and living consumption), which required land resources, thus leading to a rapid increase in LUCEs. From 2012 to 2022, the growth rate of LUCEs decreased in all counties, with smaller growth rates in the more economically developed regions of Korla City, Aksu City, Atushi City, Hotan City, Kuqa City, and Kashi City. Since 2012, China has gradually transformed the economic development model from high-speed development to high-quality development, to explore China's low-carbon economic development model [61]. The Tarim River Basin has actively responded to the national call to slow down the growth rate of LUCEs by optimizing the industrial structure and adjusting the energy structure while steadily developing the economy.

By studying the LUCE spatial correlation network structure in the Tarim River Basin from 2000 to 2022, we found that the correlation and stability of the network continued to increase, showing a decreasing trend of "core–periphery", with Aksu City, Korla City, Kashgar City, and Hotan City being located in the core's leading position, and the edge counties being located in the dominated position in the network. In addition, compared with less developed regions in China, the LUCE spatial network structure in the Tarim River Basin had distinct core and fringe regions. However, the rapid development of transportation facilities and information networks promoted the exchange of elements related to LUCEs, which brought about an increase in the mean value of gravitational force between the nodes and made the determination of specific nodes within the spatial correlation network more difficult. Compared with developed regions in China [62], the LUCE spatial correlation network in the Tarim River Basin was still relatively weak, and the development imbalance between regions was more prominent due to the low level of urbanization and population density in some regions.

4.2. Optimization of Carbon Balance Zoning

Considering the LUCE, ESC, and LUCE spatial correlation network of the Tarim River Basin, we divided the basin into six kinds of carbon balance functional zones based on the existing bases and standards for carbon balance zoning, and we put forward the following optimization proposals for each zone:

(1) Centralized carbon sink region (Aketao County): Aketao County had a large amount of carbon sink land, a high ESC, low carbon footprint pressure, a high carbon sink ecological function, and absorption of carbon overflow from other areas, and these factors were beneficial to alleviating the carbon pressure in the basin. Therefore, the future development of this region should focus on enhancing the ecological conservation function, emphasizing the protection of and increase in forest land and

grassland, strictly defining the regional development boundaries, and delineating the ecological protection zones. At the same time, relying on the rich natural resources of the county, it should promote the development of eco-tourism and facilitate the growth of environmentally friendly new industries and new modes of development.

(2) Local adjustment region (Aheqi County, Atushi City, Baicheng County, Bohu County, Cele County, Hejing County, Heshuo County, Hotan County, Koping County, Minfeng County, Pishan County, Qiemo County, Ruoqiang County, Tashkurgan Tajik Autonomous County, Yuli County, Wensu County, Wuqia County, Wushi County, Yecheng County, and Yutian County): This region, which contained relatively abundant energy resources and delivered energy to other regions with high energy dependence, showed overflow effects in the carbon emission network, thereby playing a connection role to a certain extent. In addition, the region showed high ecological pressure as it received highly energy-consuming and polluting industries transferred from economically developed regions. This region should endeavor to reduce the impact of receiving resource-intensive and high-energy-carrying industries by raising the entry thresholds for high-carbon industries, forming close interactions with developed regions to promote factors related to production and productive services, and introducing new low-carbon technologies and production methods. At the same time, the region needs to actively develop renewable and clean energy sources, such as solar, hydro, and wind, to continuously deliver renewable energy sources to counties such as Aksu, Korla, and Kashgar, which are unable to meet the economic development due to their poor resource endowment.

(3) Core–linked carbon emission region (Maigaiti County): This region's rapid economic development, dense population, and high degree of industrialization and urbanization has led to a high total volume and intensity of carbon emissions, and its local carbon sink resources were far from being able to offset carbon emissions, resulting in a serious ecological deficit. In addition to being at the center of the network, the region had a high radiating impact capacity. Therefore, the region should focus on and actively regulate its economic development model, readjust its overcrowded industrial layout based on the concept of low-carbon development, and strengthen the implementation of emission reduction measures for key industries. At the same time, the region should utilize its own radiating impact capacity to encourage the development of pilot work on carbon trading, as well as the enhancement of energy efficiency and low-carbon clean energy substitution actions, so as to bring about changes in the carbon emission behavior of surrounding areas.

(4) Dispersed–linked carbon emission region (Shufu County): This region had a large area of forest and grassland, weak intensity of human production activities, and a high amount of carbon emissions. Shufu County, located around the Kashi City, undertook the transfer of carbon emission factor resources between the Kizilsu Kyrgyz Autonomous Prefecture and the Kashi City, so it acted as a network hub in the correlation network. Therefore, the region should promote the circulation speed of low-carbon technologies by adjusting the energy consumption structure and playing the intermediary role of inter-regional synergistic emission reduction, with orientation toward the green development of industrial transformation.

(5) General–linked carbon emission region (Aksu City, Awati County, Bachu County, Jiashi County, Hotan City, Kashi City, Kuche City, Korla City, and Shaya County): In the LUCE correlation network, this region, located in a dominant position, had a siphoning effect on the inflow of labor, information technology, capital, and other factors from other regions and was the beneficiary in the network. Therefore, the region should actively adjust the optimization and upgrading of industrial structure, such as by vigorously developing tertiary and high-tech industries, reducing the development of high-energy-consuming industries, and developing more productive services and manufacturing industries based on low-carbon technologies. At the same time, the region should strengthen its advanced demonstrative role in emis-

sion reduction and energy structure transformation by capitalizing on the influence and economic radiation of the core nodes, such as Aksu City and Kashi City, and encouraging the pioneering application of mature green and low-carbon technologies, experiences, and institutional designs; this will drive the low-carbon development of the peripheral counties and help achieve effective synchronization of regional efforts to promote synergistic emission reductions.

(6) General–island carbon emission region (Luntai County, Lopu County, Moyu County, Shache County, Shule County, Xinhe County, Yanqi Hui Autonomous County, Yingjisha County, Yupu Lake County, and Zephyr County): This region, with abundant energy resources, a backward economy, remote geographical location, poor transportation infrastructure, less interaction with other counties, and weak spillover effects from other regions, took a "dominated" peripheral position in the network. Therefore, the region needs certain financial and technical support from higher-level governments to help it introduce advanced energy and low-carbon technologies and to guide it in establishing and perfecting the carbon trading market. At the same time, the region should be given appropriate preferential support from policies focusing on the establishment of channels of technological, energy, and industrial cooperation between regions at different levels of economic development so as to strengthen its spatial correlation with other regions.

Focusing on the Tarim River Basin, an oasis in an arid zone, this study revealed some differences in carbon balance zoning delineation when compared with the results of other studies. For example, in formulating a carbon-neutral zone for the Yangtze River Delta region, Du et al. considered the study area a highly economically developed region [63] and, therefore, proposed a national land optimization scheme focusing on measures such as limiting urban sprawl, controlling population densities, and optimizing the spatial structure of cities. In contrast, the Tarim River Basin has a relatively low population density, more backward industrial processes, and a large number of ecological reserves. Therefore, the pressure on carbon reduction and emission reduction is relatively small, and the national spatial optimization plan should focus on industrial transformation and ecological protection measures.

4.3. Limitations of the Study

There are two shortcomings to this study: (1) Due to the limitation of the data sources and spatial algorithms, we only studied the LUCEs of the Tarim River Basin at the county scale. In the future, we need to study the basin in more detail at lower scales and expand to other dimensions not covered in this study. (2) The carbon emission (carbon absorption) coefficients in this study were obtained by referencing previous studies. Therefore, future research should use actual carbon emission monitoring data in the basin in the calculation to improve the accuracy of the results.

5. Conclusions

By measuring the carbon source, carbon sink, and ESC of each county in the Tarim River Basin, this study used Social Network Analysis (SNA) to analyze the structure characteristics of the LUCE correlation network in the basin from 2002 to 2022, divided it into different carbon balance regions, and proposed a low-carbon development strategy for each region. The following conclusions are drawn from the results:

(1) The LUCE in the Tarim River Basin increased significantly from 1152.38 $\times$ 10^4 t in 2002 to 17,212.49 $\times$ 10^4 t in 2022. The absorption of carbon sinks was significantly lower than the emission of carbon sources, and the growth rate of carbon sources was higher than that of carbon sinks. Across the different areas, the LUCEs were relatively large in Kuche City, Korla City, Luntai County, Shaya County, and Aksu City located in the hinterland of Xinjiang. In addition, the ESC gradually decreased, showing the characteristic of "low in the middle and high at the edge".

(2) During the period 2002–2022, the spatial correlation network of LUCEs in the Tarim River Basin continued to increase in relevance and stability, with close relationships and a large scale. The spatial distribution pattern was gradually clarified, showing a decreasing trend of "core–edge", with Aksu City, Korla City, Kashgar City, and Hotan City being located in the core's leading position in the network.

(3) Based on the ESC, LUCE spatial correlation network, and exploratory spatial data analysis, the study area was divided into six types of carbon balance functional zones: a centralized carbon sink region, a local adjustment region, a core–linked carbon emission region, a dispersed–linked carbon emission region, a general–linked carbon emission region, and a general–island carbon emission region. We put forward suggestions for regionalized countermeasures to promote synergistic emission reductions.

Author Contributions: Conceptualization, J.Y.; methodology, Z.G., J.Y. and M.Z.; software and visualization, Z.G. and X.Z.; validation, Z.G. and J.Y.; formal analysis, Z.G.; investigation, Z.G., X.Z., M.L. and M.Z.; resources, Z.G.; data curation, Z.G., X.Z., H.W. and M.Z.; writing—original draft preparation, Z.G. and J.Y.; writing—review and editing, J.Y. and M.Z.; supervision, Z.G. and J.Y.; project administration, J.Y.; funding acquisition, J.Y. All authors have read and agreed to the published version of the manuscript.

Funding: This study was funded by the Social Science Foundation of China (Grant No. 23XMZ045).

Data Availability Statement: The original contributions presented in this study are included in the article. Further inquiries can be directed to the corresponding authors.

Acknowledgments: We are sincerely grateful to the editors and reviewers who commented on this paper and gave their time and effort. Finally, we would like to thank the National Social Science Foundation Committee for supporting this study.

Conflicts of Interest: The authors declare no conflicts of interest.

References

1. Huang, H.; Jia, J.; Chen, D.; Liu, S. Evolution of spatial network structure for land-use carbon emissions and carbon balance zoning in Jiangxi Province: A social network analysis perspective. *Ecol. Indic.* **2024**, *158*, 111508. [CrossRef]
2. Dutra, D.J.; Silveira, M.V.F.; Mataveli, G.; Ferro, P.D.; da Silva Magalhães, D.; de Medeiros, T.P.; Anderson, L.O.; de Aragão, L.E.d.O.e.C. Challenges for reducing carbon emissions from Land-Use and Land Cover Change in Brazil. *Perspect. Ecol. Conserv.* **2024**, *22*, 213–218. [CrossRef]
3. Gao, M. The impacts of carbon trading policy on China's low-carbon economy based on county-level perspectives. *Energy Policy* **2023**, *175*, 113494. [CrossRef]
4. Fan, Y.; Wang, Y.; Han, R.; Li, X. Spatial-Temporal Dynamics of Carbon Budgets and Carbon Balance Zoning: A Case Study of the Middle Reaches of the Yangtze River Urban Agglomerations, China. *Land* **2024**, *13*, 297. [CrossRef]
5. Fattah, M.A.; Morshed, S.R.; Morshed, S.Y. Impacts of land use-based carbon emission pattern on surface temperature dynamics: Experience from the urban and suburban areas of Khulna, Bangladesh. *Remote Sens. Appl. Soc. Environ.* **2021**, *22*, 100508. [CrossRef]
6. Gao, F.; He, Z. Digital economy, land resource misallocation and urban carbon emissions in Chinese resource-based cities. *Resour. Policy* **2024**, *91*, 104914. [CrossRef]
7. Xia, C.; Zhang, J.; Zhao, J.; Xue, F.; Li, Q.; Fang, K.; Shao, Z.; Li, S.; Zhou, J. Exploring potential of urban land-use management on carbon emissions—A case of Hangzhou, China. *Ecol. Indic.* **2023**, *146*, 109902. [CrossRef]
8. Zhang, X.; Fan, H.; Hou, H.; Xu, C.; Sun, L.; Li, Q.; Ren, J. Spatiotemporal evolution and multi-scale coupling effects of land-use carbon emissions and ecological environmental quality. *Sci. Total Environ.* **2024**, *922*, 171149. [CrossRef]
9. Cai, C.; Fan, M.; Yao, J.; Zhou, L.; Wang, Y.; Liang, X.; Liu, Z.; Chen, S. Spatial-temporal characteristics of carbon emissions corrected by socio-economic driving factors under land use changes in Sichuan Province, southwestern China. *Ecol. Inform.* **2023**, *77*, 102164. [CrossRef]
10. Liu, S.; Jia, J.; Huang, H.; Chen, D.; Zhong, Y.; Zhou, Y. China's CO2 emissions: A thorough analysis of spatiotemporal characteristics and sustainable policy from the agricultural land-use perspective during 1995–2020. *Land* **2023**, *12*, 1220. [CrossRef]
11. Song, C.; Yang, J.; Wu, F.; Xiao, X.; Xia, J.; Li, X. Response characteristics and influencing factors of carbon emissions and land surface temperature in Guangdong Province, China. *Urban Clim.* **2022**, *46*, 101330. [CrossRef]
12. Luo, H.; Liu, Z.; Li, Y.; Meng, X.; Yang, X. Characterizing and predicting carbon emissions from an emerging land use perspective: A comprehensive review. *Urban Clim.* **2024**, *58*, 102141. [CrossRef]

13. Luo, H.; Li, Y.; Gao, X.; Meng, X.; Yang, X.; Yan, J. Carbon emission prediction model of prefecture-level administrative region: A land-use-based case study of Xi'an city, China. *Appl. Energy* **2023**, *348*, 121488. [CrossRef]
14. Zhang, X.; Zhang, D. Urban carbon emission scenario prediction and multi-objective land use optimization strategy under carbon emission constraints. *J. Clean. Prod.* **2023**, *430*, 139684. [CrossRef]
15. Zhu, K.; Cheng, Y.; Zhou, Q.; Azadi, H. Understanding Future Water-Carbon-Land Coupled Systems in the Era of COP 27: The Case of the Hanjiang River Basin, China. *J. Clean. Prod.* **2024**, *479*, 144054. [CrossRef]
16. Bastos, A.; Hartung, K.; Nützel, T.B.; Nabel, J.E.; Houghton, R.A.; Pongratz, J. Comparison of uncertainties in land-use change fluxes from bookkeeping model parameterisation. *Earth Syst. Dyn.* **2021**, *12*, 745–762. [CrossRef]
17. Choi, S.E.; Hong, S.; Song, C.; Kim, J.; Kim, W.; Ha, R.; Lee, W.K. Construction of land-use change matrix and estimation of greenhouse gas inventory focusing on settlements in South Korea. *Carbon Balance Manag.* **2023**, *18*, 4. [CrossRef]
18. Gui, D.; He, H.; Liu, C.; Han, S. Spatio-temporal dynamic evolution of carbon emissions from land use change in Guangdong Province, China, 2000–2020. *Ecol. Indic.* **2023**, *156*, 111131. [CrossRef]
19. Niu, H.; Chen, S.; Xiao, D. Multi-Scenario land cover changes and carbon emissions prediction for peak carbon emissions in the Yellow River Basin, China. *Ecol. Inform.* **2024**, *168*, 112794. [CrossRef]
20. Yang, Y.; Li, H. Monitoring spatiotemporal characteristics of land-use carbon emissions and their driving mechanisms in the Yellow River Delta: A grid-scale analysis. *Environ. Res.* **2022**, *214*, 114151. [CrossRef]
21. Li, J.; Huang, X.; Chuai, X.; Yang, H. The impact of land urbanization on carbon dioxide emissions in the Yangtze River Delta, China: A multiscale perspective. *Cities* **2021**, *116*, 103275. [CrossRef]
22. Rong, T.; Zhang, P.; Zhu, H.; Jiang, L.; Li, Y.; Liu, Z. Spatial correlation evolution and prediction scenario of land use carbon emissions in China. *Ecol. Inform.* **2022**, *71*, 101802. [CrossRef]
23. Yu, Z.; Chen, L.; Tong, H.; Chen, L.; Zhang, T.; Li, L.; Yuan, L.; Xiao, J.; Wu, R.; Bai, L.; et al. Spatial correlations of land-use carbon emissions in the Yangtze River Delta region: A perspective from social network analysis. *Ecol. Indic.* **2022**, *142*, 109147. [CrossRef]
24. Carpio, A.; Ponce-Lopez, R.; Lozano-García, D.F. Urban form, land use, and cover change and their impact on carbon emissions in the Monterrey Metropolitan area, Mexico. *Urban Clim.* **2021**, *39*, 100947. [CrossRef]
25. Li, J.; Jiao, L.; Li, F.; Lu, X.; Hou, J.; Li, R.; Cai, D. Spatial disequilibrium and influencing factors of carbon emission intensity of construction land in China. *J. Clean. Prod.* **2023**, *396*, 136464. [CrossRef]
26. Li, W.; Chen, Z.; Li, M.; Zhang, H.; Li, M.; Qiu, X.; Zhou, C. Carbon emission and economic development trade-offs for optimizing land-use allocation in the Yangtze River Delta, China. *Ecol. Indic.* **2023**, *147*, 109950. [CrossRef]
27. Chen, X.; Di, Q.; Jia, W.; Hou, Z. Spatial correlation network of pollution and carbon emission reductions coupled with high-quality economic development in three Chinese urban agglomerations. *Sustain. Cities Soc.* **2023**, *94*, 104552. [CrossRef]
28. Bai, C.; Zhou, L.; Xia, M.; Feng, C. Analysis of the spatial association network structure of China's transportation carbon emissions and its driving factors. *J. Environ. Manag.* **2020**, *253*, 109765. [CrossRef]
29. Wang, Y.; Zhou, Y.; Wu, S.; Peng, X. Colonize the desert vs. retreat to the mountains: The evolution of city-water relationships in the Tarim river basin over the past 2000 years. *Appl. Geogr.* **2024**, *170*, 103346. [CrossRef]
30. Cui, X.; Liu, X.; Liang, A.; Chen, G.; Li, T.; Yang, X.; Zhang, Z.; Dong, Z. Desert-oasis evolutionary process in the Tarim Basin since∼ 2.2 ka BP during the late Holocene and their environmental implications. *Catena* **2024**, *246*, 108381. [CrossRef]
31. Wu, Y.; Tam, V.W.; Shuai, C.; Shen, L.; Zhang, Y.; Liao, S. Decoupling China's economic growth from carbon emissions: Empirical studies from 30 Chinese provinces (2001–2015). *Sci. Total Environ.* **2019**, *656*, 576–588. [CrossRef] [PubMed]
32. Xu, M.; Zhang, S.; Li, P.; Weng, Z.; Xie, Y.; Lan, Y. Energy-related carbon emission reduction pathways in Northwest China towards carbon neutrality goal. *Appl. Energy* **2024**, *358*, 122547. [CrossRef]
33. Kulaixi, Z.; Chen, Y.; Wang, C.; Xia, Q. Spatial differentiation of ecosystem service value in an arid region: A case study of the Tarim River Basin, Xinjiang. *Ecol. Indic.* **2023**, *151*, 110249. [CrossRef]
34. Feng, M.; Chen, Y.; Duan, W.; Zhu, Z.; Wang, C.; Hu, Y. Water-energy-carbon emissions nexus analysis of crop production in the Tarim river basin, Northwest China. *J. Clean. Prod.* **2023**, *396*, 136566. [CrossRef]
35. Zhang, J.; Hao, X.; Li, X.; Fan, X.; Zhang, S. Evaluation and regulation strategy for ecological security in the Tarim River Basin based on the ecological footprint. *J. Clean. Prod.* **2024**, *435*, 140488. [CrossRef]
36. Song, J.; Aishan, T.; Ma, X. Coupled water-habitat-carbon nexus and driving mechanisms in the Tarim River Basin: A multi-scenario simulation perspective. *Ecol. Indic.* **2024**, *167*, 112649. [CrossRef]
37. Yao, J.; Chen, Y.; Guan, X.; Zhao, Y.; Chen, J.; Mao, W. Recent climate and hydrological changes in a mountain–basin system in Xinjiang, China. *Earth-Sci. Rev.* **2022**, *226*, 103957. [CrossRef]
38. Li, Y.; Kong, L.; Ma, L.; Zeng, T.; Liu, W.; Abuduwaili, J. Deciphering the driving factors and probabilistic health risks of potentially toxic elements in arid surface water: Insights from the Tarim River Basin. *Ecotoxicol. Environ. Saf.* **2024**, *286*, 117211. [CrossRef]
39. Ariken, M.; Zhang, F.; Chan, N.; Kung, H. Coupling coordination analysis and spatio-temporal heterogeneity between urbanization and eco-environment along the Silk Road Economic Belt in China. *Ecol. Indic.* **2021**, *121*, 107014. [CrossRef]
40. Zhang, N.; Sun, F.; Hu, Y. Carbon emission efficiency of land use in urban agglomerations of Yangtze River Economic Belt, China: Based on three-stage SBM-DEA model. *Ecol. Indic.* **2024**, *160*, 111922. [CrossRef]
41. Wang, Q.; Yang, C.; Wang, L.; Zhao, L.; Zhao, Y.; Zhang, Q.; Zhang, C. Decoupling analysis to assess the impact of land use patterns on carbon emissions: A case study in the Yellow River Delta efficient eco-economic zone, China. *J. Clean. Prod.* **2023**, *412*, 137415. [CrossRef]

42. Chen, J.; Gao, M.; Cheng, S.; Hou, W.; Song, M.; Liu, X.; Liu, Y.; Shan, Y. County-level CO_2 emissions and sequestration in China during 1997–2017. *Sci. Data* **2020**, *7*, 391. [CrossRef] [PubMed]
43. Bai, J.; Chen, H.; Gu, X.; Ji, Y.; Zhu, X. Temporal and spatial characteristics of carbon emissions from cultivated land use and their influencing factors: A case study of the Yangtze River Delta region. *Int. Rev. Econ. Financ.* **2024**, *96*, 103501. [CrossRef]
44. Zhang, L.; Pang, J.; Chen, X.; Lu, Z. Carbon emissions, energy consumption and economic growth: Evidence from the agricultural sector of China's main grain-producing areas. *Sci. Total Environ.* **2019**, *665*, 1017–1025. [CrossRef] [PubMed]
45. Ning, J.; Wang, Z.; Du, G.; Li, Y. Characteristics of agricultural carbon emissions in northeast China and its eecoupling state with agricultural economy. *Econ. Geogr.* **2023**, *43*, 173–180.
46. Tang, H.; Ma, H.; Su, Y.; Xin, C.; Wang, J. Carbon emissions and carbon absorptions of different land use types in Xinjiang. *Arid Zone Res.* **2016**, *33*, 486–492.
47. Su, Y.; Ma, H.; Li, F. Xinjiang agriculture and animal husbandry carbon emissions andits decoupling relationship with agricultural economic growth. *Arid Land Geogr.* **2014**, *37*, 1047–1054.
48. Deng, L.; Yuan, S.; Bai, P.; Li, H. Evaluation of agricultural carbon emissions in Xinjiang and analysis of driving factors based on machine learning algorithms. *Chin. J. Eco-Agric.* **2023**, *31*, 265–279.
49. Wei, B.; Alimujiang, K.; Reheman, R.; Zhang, X.; Zhao, Y.; Aizizi, Y.; Liang, H. Spatiotemporal characteristics and prediction of carbon emissions/absorption from land use change in the urban agglomeration on the northern slope of the Tianshan Mountains. *Ecol. Indic.* **2023**, *151*, 110329. [CrossRef]
50. Jin, D.; Liu, X. Comprehensive svaluation and analysis of carbon emissions from land use in 14 cities in Xinjiang from 2005 to 2020. *Adm. Tech. Environ. Monit.* **2023**, *36*, 15–20.
51. Zhang, R.; Li, P.; Xu, L. Effects of urbanization on carbon emission from land use in Xinjiang and their coupling relationship. *Acta Ecol. Sin.* **2022**, *42*, 5226–5242.
52. Ye, C.; Ming, T. Land use carbon emissions estimation and carbon emissions control strategy effect scenario simulation in Zhejiang province. *Heliyon* **2023**, *9*, e20783. [CrossRef]
53. Farine, D.R.; Whitehead, H. Constructing, conducting and interpreting animal social network analysis. *J. Anim. Ecol.* **2015**, *84*, 1144–1163. [CrossRef] [PubMed]
54. Peng, F. Economic spatial connection and spatial structure of Guangdong-Hong Kong-Macao Greater Bay and the surrounding area cities—An empirical analysis based on Improved Gravity Model and Social Network Analysis. *Econ. Geogr.* **2015**, *35*, 50–56.
55. Wei, Y.; Chen, S. Spatial correlation and carbon balance zoning of land use carbon emissions in Fujian Province. *Acta Ecol. Sin.* **2021**, *41*, 5814–5824.
56. Kim, J.; Hastak, M. Social network analysis: Characteristics of online social networks after a disaster. *Int. J. Inf. Manag.* **2018**, *38*, 86–96. [CrossRef]
57. Sun, L.; Qin, L.; Taghizadeh-Hesary, F.; Zhang, J.; Mohsin, M.; Chaudhry, I.S. Analyzing carbon emission transfer network structure among provinces in China: New evidence from social network analysis. *Environ. Sci. Pollut. Res.* **2020**, *27*, 23281–23300. [CrossRef]
58. Wang, Z.; Xie, W.; Zhang, C. Towards COP26 targets: Characteristics and influencing factors of spatial correlation network structure on US carbon emission. *Resour. Policy* **2023**, *81*, 103285. [CrossRef]
59. Sporkmann, J.; Liu, Y.; Spinler, S. Carbon emissions from European land transportation: A comprehensive analysis. *Transp. Res. Part D Transp. Environ.* **2023**, *121*, 103851. [CrossRef]
60. Zhu, R.; Liu, W.; Xue, R.; Teng, S.; Wang, Y.; Pan, Y.; Gao, W. Linking wilderness mapping and ecosystem services: Identifying integrated wilderness and ecological indicators to quantify ecosystem services of wilderness. *Ecol. Indic.* **2024**, *160*, 111915. [CrossRef]
61. Li, Y.; Wei, W.; Zhou, J.; Hao, R.; Chen, D. Changes in land use carbon emissions and coordinated zoning in China. *Environ. Sci.* **2023**, *44*, 1267–1276.
62. Xing, X.; Li, X.; Huang, X.; Liu, X.; Wei, J. Study on evolution of spatial characteristics of land use carbon emission in China. *Resour. Dev. Mark.* **2021**, *66*, 102701.
63. Du, H.; Yang, S.; Li, Z.; Guo, Z.; Fan, Q. Spatio-temporal characteristics and influencing factors of carbon sources/sinks in the Yangtze River Delta under carbon neutrality target. *Environ. Sci.* **2024**, 1–13. [CrossRef]